

## About the effects of an oscillating miniflap upon the wake on an airfoil, all immersed in turbulent flow

Delnero, J. S.<sup>1,2,\*</sup>; Marañón Di Leo, J.<sup>1,2</sup>; Colman, J.<sup>1</sup>; Camocardi, M.<sup>1,2</sup>; García Sainz, M.<sup>1,3</sup> & Muñoz, F.<sup>1,3</sup>

<sup>1</sup>LaCLyFA, Departamento Aeronáutica, Facultad de Ingeniería, Universidad Nacional de La Plata, Argentina

<sup>2</sup>Conicet, Avda. Rivadavia 1917, CP C1033AAJ, Ciudad. de Buenos Aires, Argentina.

<sup>3</sup>Comisión de Investigaciones Científicas de la Pcia. de Bs. As., 526 y 10, CP 1899, La Plata

E-mail: delnero@ing.unlp.edu.ar

**Abstract.** The present research analyzes the asymmetry in the rolling up shear layers behind the blunt trailing edge of an airfoil 4412 with a miniflap acting as active flow control device and its wake organization. Experimental investigations relating the asymmetry of the vortex flow in the near wake region, able to distort the flow increasing the downwash of an airfoil, have been performed. All of these in a free upstream turbulent flow (1.8% intensity). We examine the near wake region characteristics of a wing model with a 4412 airfoil without and with a rotating miniflap located on the lower surface, near the trailing edge. The flow in the near wake, for 3 x-positions (along chord line) and 20 vertical points in each x-position, was explored, for three different rotating frequencies, in order to identify signs of asymmetry of the initial counter rotating vortex structures. Experimental evidence is presented showing that for typical lifting conditions the shear layer rollup process within the near wake is different for the upper and lower vortices: the shear layer separating from the pressure side of the airfoil begins its rollup immediately behind the trailing edge, creating a stronger vortex while the shear layer from the suction side begins its rollup more downstream creating a weaker vortex. The experimental data were processed by classical statistics methods. Aspects of a mechanism connecting the different evolution and pattern of these initial vortex structures with lift changes and wake alleviating processes, due to these miniflaps, will be studied in future works.

### 1. Introduction

The wake immediately behind a common lifting airfoil is asymmetric due to the different external and boundary layer flows on the pressure and suction surfaces of the airfoil. The wake structure in this near wake region is influenced by aero dynamical loading and airfoil characteristics. Downstream of the trailing edge of a normal lifting airfoil the downwash diminishes rapidly. Hah and Lakshminarayana (1982), in their experimental and numerical study about the near wake of a lifting airfoil, confirmed that the asymmetric wake becomes nearly symmetric after only one chord length downstream of the trailing edge. These authors reported also that the far wake shows a roughly symmetric wake structure in which the airfoil features and aero dynamical loading do not influence the wake development anymore. The main downwash occurs within the asymmetric region. A miniflap like Gurney type is a plate located on the lower surface of the wing, along the wingspan, with a height between 1% and 2% of the wing chord. Despite a long-standing experience in the classic lift

evaluation due to a vortex system bound to a wing, the unsteady nature of the counter rotating vortices behind a Gurney flap complicates a physical realistic theoretical understanding of the lift increase generated by these miniflaps (Li et al, 2002; Myose, 1998). It is known that the highly unsteady nature of flows associated with vortex shedding make difficult its theoretical and experimental understanding. It should be mentioned that up to date there are no theories for predicting the drag coefficient as a function of Reynolds number in vortex shedding conditions of extremely basic bodies as a circular cylinders. These types of flaps were studied by many authors [Liebeck, 1978; Neuhart & Pendergraft, 1988; Bloy & Durrant, 1995; Storm & Jang, 1994; Giguère et al, 1995], reporting an increase of the lift and lift-to-drag ratio and a reduced form drag obtained at high lift coefficients compared with the same airfoil without the flap. Giguère et al. (1995) described experimentally the aerodynamic behaviour of these flaps scaling their height with the boundary layer thickness near the trailing edge. These authors conjectured that the trailing edge counter-rotating vortices induce streamlines resembling a smooth aerodynamic prolongation of the airfoil, allowing a better trailing edge pressure recovery, adding a virtual camber by shifting downward the Kutta condition. A more detailed description of the flow structures in the Gurney flap pattern obtained by experiments with laser Doppler anemometry (LDA) was reported. Aspects of the behaviour of airfoils equipped with miniflaps with different lengths were described by Bacchi et al (2006), reported about the influence of free stream turbulence structure on these devices. Going far, mini-flaps acting on the lower surface of the wing could contribute to overcome stall even at high angles of attack. This feature is very important not only for airplanes but also for wind turbines rotor blades. Nevertheless, the majority of the authors didn't explore the fluid dynamic pattern around the airfoil, in particular the near wake - being at low or high angles of attack - when the airfoil is immersed in a turbulent stream, which intensity is between 1% to 2%, like the low atmospheric turbulent boundary layer over plain terrain, in which the airplanes land and takeoff; UAVs fly; wind turbines operate; etc. Also, many of the authors explore the use of miniflaps as passive flow control devices. In that sense, the aim of our work is to analyze the wake modulation by a rotating miniflap (active flow control device), under a turbulent upstream flow, the relation of the characteristics of such wake with the variable rotating frequency of the flap and how such flow pattern could affect the airfoil's circulation, the overall resulted wake pattern and the possible lift enhancement. In this way, we proposed to study the near wake downstream the airfoil with the Gurney flap fixed and oscillating, at 1h, 2h and 5h distance from the trailing edge, analyzing the Spectra, the temporal and spatial scales (Hinze, 1975).

## 2. Experimental procedure

The experiments were carried out in the closed section boundary layer wind tunnel of 1.4mx1m cross section, which belongs to the Boundary Layer & Environmental Fluid Dynamics Laboratory (Engineering Faculty, National University of La Plata, Argentina). The tested model was an untwisted wing with NACA 4412 airfoil, of 80cm wingspan and 50cm chord (c), bounded by two big double plates in order to assure a 2D flow over it (see Figures 1 and 2). The upstream flow had 1.8% turbulence intensity, and the experiments were performed for an upstream mean velocity of 10m/s. The Reynolds number, based upon the wing chord and the mean free stream velocity (measured at 1.5m ahead the model at its height) was 489000. The turbulence intensity was 1.8% (minimum turbulence intensity of the wind tunnel). Inside the wing model there was an electromechanical device capable to bring a rotating movement (see Figure 1) to a mini-flap, around its wingspan axe up to 30° from the airfoil chord, being the mini-flap height  $h = 1.5\%c$ . The rotating frequencies were 22Hz, 38Hz and 44Hz. The experiments were focused on the instantaneous velocity measurements in the near wake, in three "x" positions, 1h, 2h and 5h and, at each "x" position, the data were measured in 20 vertical points, which upper limit was  $1.5\%c$  and lower limit  $2\%c$ , separated each  $0.04\%c$ . The procedure was: 1<sup>st</sup> step with the clean model; 2<sup>nd</sup> step with the flap deployed but fixed (as a passive flow control device); 3<sup>rd</sup> step with the flap oscillating at the three frequencies already mentioned. In all cases at  $0^\circ$  angle of attack. See Figure 3 for the sketch of the measurements positions and Figure 4 for

the front view of the model, between the two plates, inside test section. We measured instantaneous velocities in such points. The acquisition frequency was 4000 Hz, filtered at 1000Hz, taken 8192 samples per channel in each measuring point. The flaps frequencies were measured with a laser tachometer. The aim of the experiments was to find a mini-flap frequency or group of frequencies favorable to manipulate the airfoil's wake in the sense to down the Kutta condition and to looking for, in the future, changes in the lift, shifting stall to higher angles of attack, and achieving also better aerodynamic efficiencies.

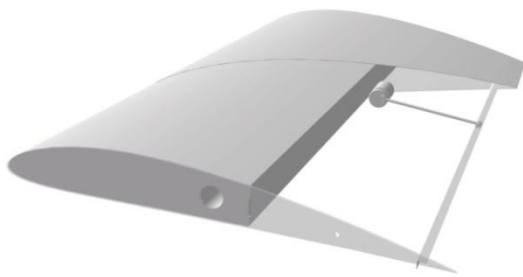


Figure 1. Tested wing model with rotational oscillation mini-flap Gurney

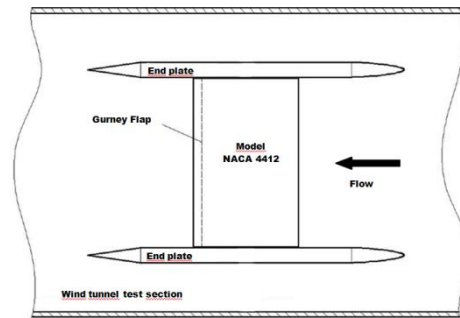


Figure 2. Sketch of the wing model inside the wind tunnel test section

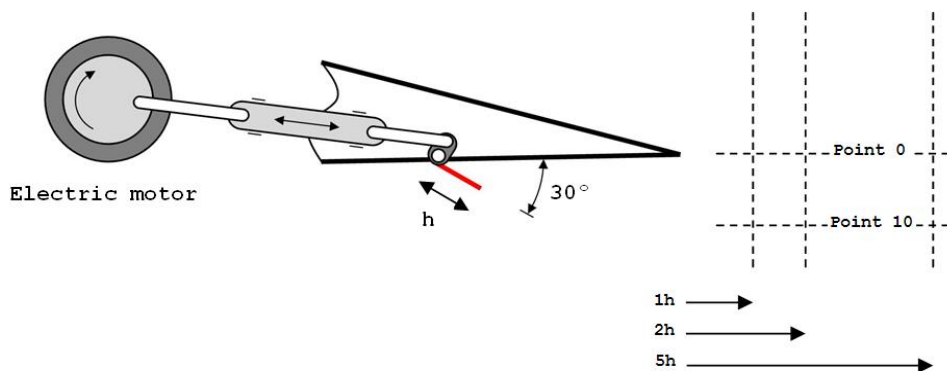


Figure 3. Wake measurements sketch for the rotating-oscillating mini-flap Gurney



Figure 4. Front view of the model inside test section

The purpose to measure with some detail the near wake is to try to identify asymmetrical vortex structures closely related with a shift down of the rear stagnation point (Kutta condition), promoted by the miniflap action.

### 3. Results

We displayed part of the huge instantaneous velocity measurements, with the aim to explore qualitatively and quantitatively the particular fluid dynamic pattern, promoted by the flap oscillations, in the near wake region, as a consequence of the active flow control of such device upon the airfoil's aerodynamic characteristics. We observed the almost perfect match between the flap oscillating frequencies and the special wake structure, with a peak at the same frequency than the oscillating one and other peaks which are other structures, not harmonics because they aren't multiples of the first (fundamental). In order to support such assumptions, we also showed the corresponding velocities spectra at some selected vertical points (Figures 5) and the horizontal and vertical velocities components on each "x" position (1h, 2h and 5h) for all the vertical points (mean free stream of 10m/s and  $0^\circ$  angle of attack)(Figure 6).

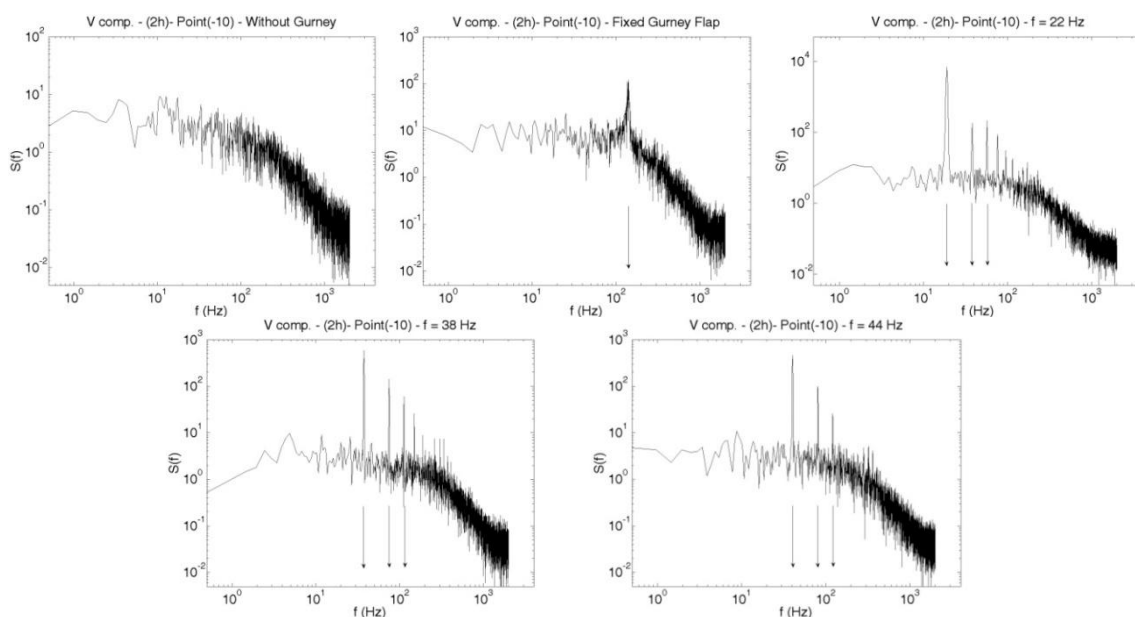


Figure 5. V component velocities spectra, for the clean airfoil, fixed Gurney and moving one (three frequencies), 2h x-position and vertical point -10.

The spectra peaks, showed in Figure 5, were as follows: For 22 Hz (oscillating frequency), first peak at 22 Hz and successively (approximate) 39 Hz, 58 Hz, 74 Hz, 92 Hz and 110 Hz; for 38 Hz (oscillating frequency), the peaks were at 30 Hz, 78 Hz, 110 Hz, 124 Hz, 190 Hz; for 44 Hz (oscillating frequency), the peaks were 44 Hz, 82 Hz, 108 Hz. For the fixed GF condition, the peak was at 142 Hz. One could see how the oscillation of the mini-flap made important changes on the wake characteristics. The periodic (coherent) vortex street, generated by the oscillating mini-flap, had enough strength to overlap and diminish the intensity of the turbulent structures typical of the airfoil with the fixed mini-flap. This behaviour is more significantly as the oscillating frequency grows. In that way, important changes in the wake, promoted by the oscillating mini-flap, will affect directly the general circulation around the airfoil. Thus, our main concern is to measure the near wake with some detail. We could see how the turbulent intervals between peaks, are reduced as the oscillating frequency grows. This is due, probably, to the fact that once we overcome some frequency step, the characteristics of the periodic structures, shed by the oscillating mini-flap, become almost independent of the frequency and, so, the near wake structure will be similar for frequencies above such step.

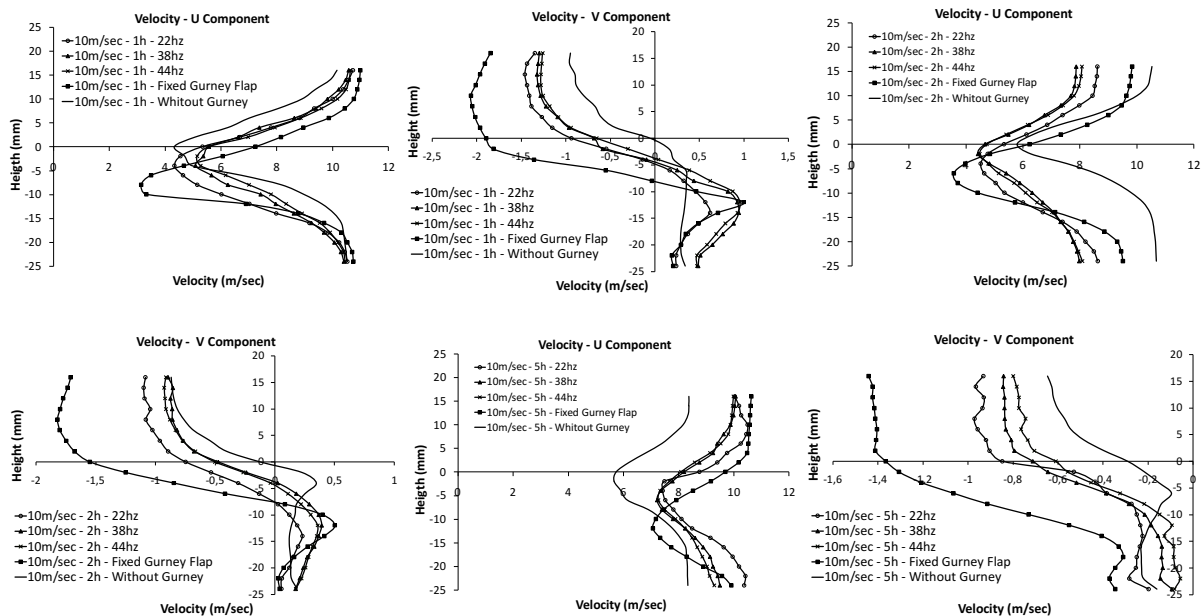


Figure 6. Horizontal and vertical mean velocities at 1h, 2h and 5h behind the trailing edge, for the three oscillating frequencies (0 degree angle of attack).

Examination of Figure 6, following the three “x” positions, suggest the formation of a pair of vortices, one anticlockwise close to the trailing edge, generated by the miniflap and the other, clockwise, following the first, probably due the flow from the upper surface of the airfoil. This asymmetry was detected by other authors, but mainly for the fixed miniflap case. We could conclude that, for both “x” positions 1h and 2h, the U-component has small changes between the different conditions (clean airfoil; fixed flap; etc), being always positive above and below the trailing edge, but with a reduction of its magnitude from the trailing edge level to the end of mini-flap level. The vertical velocities exhibit important differences, above the trailing edge, between the clean airfoil and the fixed mini-flap cases. For the 5h case, the clockwise vortex structure is clear, probably produced by the flow that comes from the upper surface of the airfoil. Respect the oscillating mini-flap, there are small differences between the vertical velocities for the three frequencies but, if we look close the vertical velocities at the mini-flap level and lower, their values are greater than the corresponding to clean airfoil or even the fixed mini-flap case. It’s clear that we have an anticlockwise vortex behind the mini-flap. This is consistent with the results founded by other authors [Liebeck, 1978; Neuhart & Pendergraft, 1988; Bloy & Durrant, 1995; Storm & Jang, 1994; Myose et al, 1998; Van Dam et al, 1999; Gai & Palfrey, 2003; Boldes et al, 2008; Tang & Dowel, 2007; Zhan & Wang, 2004; Matalanis & Eaton, 2007]. At this stage, in order to add information that help to characterize the fine structure of the turbulence at the near wake, and bearing in mind the big quantity of data available, in order to simplify we proceed to calculate the autocorrelation function and the power density spectrum, of the two velocity components at two representative vertical positions in each “x” position for one angle of attack value:  $0^{\circ}$ . This will be enough to achieve a “picture” of the spatial turbulent scales (provided Taylor hypothesis is satisfied) and the corresponding energy distribution. The following Tables (Table 1, Table 2 and Table 3) indicate the configuration for the different downstream “x” positions (1h, 2h and 5h); the first cut (in the graphic C(t) vs. time) (see figure 7), on the time coordinate for the u-component ( $t_{cu}$ ) and the v-component ( $t_{cv}$ ); period (T); frequency (F: Hertz).

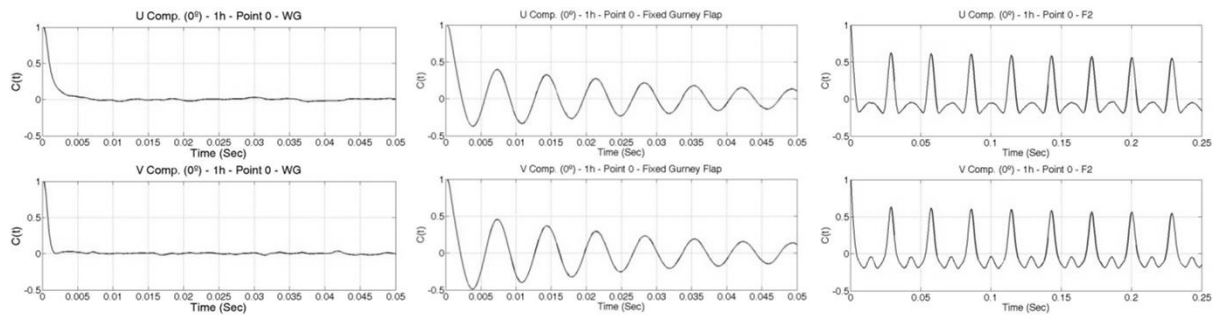


Figure 7 The autocorrelation coefficient vs time

Table 1. Wake configuration for a distance 1h downstream the trailing edge

Configuration	tcu (seg)	tcv (sec)	U (m/sec)	V (m/sec)	Eu (m)	Ev (m)	T (sec)	F (Hz)	F (exp) Hz	S(f)v	S(f)u
0° 1h point 0 - PS	0,0073	0.002	4.329	-0.051	0.031602	-0.0001	-	-	-	-	-
0° 1h point -10 - PS	0.0372	0.002	8.969	0.351	0.333647	0.000702	-	-	-	-	-
0° 1h point 0 - GF	0.0023	0.0021	7.236	-1.899	0.016643	-0.00399	-	-	141.6	160.7	187.6
0° 1h point -10 - GF	0.00317	0.00226	3.328	0.466	0.01055	0.001053	-	-	140.1	25.51	23.21
0° 1h point -10 - F1	0.0154	0.00794	6.014	0.459	0.092616	0.003644	0.06	16.66	16.6	170.5	11740
0° 1h point -10 - F2	0.00694	0.00324	7.425	0.822	0.05153	0.002663	0.0282	35.46	36.13	1243	1731
0° 1h point -10 - F3	0.0062	0.00307	7.797	0.875	0.048341	0.002686	0.0246	40.65	41.02	1628	1410
0° 1h point -0 - F1	0.0135	0.014	5.342	-0.935	0.072117	-0.01309	0.0607	16.47	16.6	1253	1127
0° 1h point -0 - F2	0.0039	0.00428	5.571	-0.683	0.021727	-0.00292	0.0286	34.96	35.16	848.3	820
0° 1h point -0 - F3	0.0032	0.00337	5.565	-0.652	0.017808	-0.0022	0.0245	40.81	41.02	620	582

Table 2. Wake configuration for a distance 2h downstream the trailing edge

Configuration	tcu (sec)	tcv (sec)	U (m/sec)	V (m/sec)	Eu(m)	Ev(m)	T (sec)	F (Hz)	F(ex p) Hz	S(f)v	S(f)u
0° 2h point 0 - PS	0.0114	0.00919	5.795	-0.123	0.066063	-0.00113	-	-	-	-	-
0° 2h point -10 - PS	0.03273	0.0068	9.809	0.17	0.321049	0.001156	-	-	-	-	-
0° 2h point 0 - GF	0.00223	0.00197	6.28	-1.548	0.014004	-0.00305	-	-	140.1	159.8	136
0° 2h point -10 - GF	0.00235	0.00209	4.416	0.4	0.010378	0.000836	-	-	137.2	254	113.3
0° 2h point -10 - F1	0.01329	0.00282	5.353	0.12	0.071141	0.000338	0.0528	18.94	19.04	52.37	7001
0° 2h point -10 - F2	0.00631	0.00244	6.331	0.369	0.039911	0.0009	0.0268	37.31	37.6	649.7	609.3
0° 2h point -10 - F3	0.00588	0.00236	6.089	0.302	0.035803	0.000714	0.025	40	40.53	513.4	477.7
0° 2h point -0 - F1	0.01317	0.0132	5.338	-0.747	0.070301	-0.00986	0.054	18.51	18.55	744.6	583.6
0° 2h point -0 - F2	0.00316	0.00337	4.681	-0.474	0.014797	-0.0016	0.02675	37.38	38.09	412.5	215.9
0° 2h point -0 - F3	0.00289	0.00312	4.734	-0.501	0.013686	-0.00156	0.025	40	40.53	404.6	197.3

Table 3. Wake configuration for a distance 5h downstream the trailing edge

Configuration	tcu (seg)	tev (seg)	U (m/sec)	V (m/sec)	Eu(m)	Ev(m)	T (sec)	F (Hz)	F (exp) Hz	S(f)v	Sfu
0° 5h point 0 - PS	0.039	0.001858	5.736	-0.29	0.223704	-0.00054	-	-	-	-	-
0° 5h point -10 - PS	0.03213	0.001685	7.393	-0.161	0.237537	-0.00027	-	-	-	-	-
0° 5h point 0 - GF	0.00233	0.00198	9.697	-1.366	0.022633	-0.0027	-	-	145.5	266.1	202.3
0° 5h point -10 - GF	0.002355	0.002085	7.173	-0.731	0.016892	-0.00152	-	-	143.1	538.9	41.36
0° 5h point -10 - F1	0.001384	0.00294	8.104	-0.25	0.011216	-0.00074	0.0543	18.41	18.55	72.48	4051
0° 5h point -10 - F2	0.002378	0.002347	7.799	-0.215	0.018546	-0.0005	0.0275	36.36	36.62	378.6	65.11
0° 5h point -10 - F3	0.002503	0.002272	7.894	-0.147	0.019759	-0.00033	0.0234	42.73	43.46	241.6	146.3
0° 5h point -0 - F1	0.01333	0.00834	8.754	-0.847	0.116691	-0.00706	0.0548	18.24	18.55	467	901.9
0° 5h point -0 - F2	0.004213	0.00379	8.197	-0.712	0.034534	-0.0027	0.0274	36.49	36.62	623.9	599.7
0° 5h point -0 - F3	0.003188	0.003075	8.086	-0.61	0.025778	-0.00188	0.0235	42.55	42.97	343.8	187.7

From the analysis of the Table's data, at the trailing edge level, for example (vertical point "0"), 1h and 2h "x" positions, the turbulence horizontal and vertical macro scales diminish from the clean airfoil to the fixed mini-flap case and, for the moving mini-flap, such spatial scale diminishes more as frequency grows. These results are consistent with the horizontal and vertical mean velocity components showed in Figure 6, for all the situations: clean airfoil; fixed mini-flap; rotating mini-flap (three frequencies). For 5h "x" position is observed a little increment of the horizontal macro scale from the clean airfoil to the fixed miniflap situation, but remains the tendency to diminish both macro scales for the moving miniflap as frequency grow. Observing the vertical point -10 at the 1h "x" position, it's clear that the horizontal macro scales diminish meanwhile the vertical ones augment. Moreover, for that point, both horizontal and vertical scales are bigger than the fixed and clean cases, but they lowering as frequency go up. By other way, at 2h "x" position, the horizontal and vertical macro scales diminish from the clean airfoil to the fixed miniflap but, for the moving one, the horizontal and vertical macro scales are bigger than the fixed miniflap and also lowering as frequency grow. Nevertheless, for the 5h "x" position, the behaviour for the moving miniflap, regarding the horizontal macro scale, is the opposite than the previous "x" positions. Meanwhile, the vertical macro scale preserves its lowering tendency as in the previous "x" positions. From the point of view of the density power spectrum of the first forced peak, the energy associated with the vertical velocities augment as the frequency increase, at the tested vertical point -10 (at the miniflap width level), being such behaviour the opposite at the point 0 (at the trailing edge level), for 1h, 2h and 5h "x" positions. In fact, if we observe carefully the energy evolution, there are an augment from the lower frequency to the 2<sup>nd</sup> and then a small decrement of it. On explaining such behaviour we must take in account that the analysis was made following the flow evolution at fixed reference points instead to "follow" the vortex structures and, so, due the mix between the upper and lower flows will grow as we go far from the trailing edge, probable the energy augment for the middle frequency is due such mix.

#### 4. Conclusions

From the Tables analysis, we could say that as miniflap frequency go up the vortex structures by it generated become small and, subsequently, the associated energy will diminish. In particular, the vertical velocities of the vortex structures generated by the moving miniflap will diminish as the frequency grows and, so, the resultant vertical velocity of the flow, in the near wake region, will decay as the frequency augments. This implies, a downwash lowering with frequency and, probably, this could affect negatively the Kutta condition down shift. Nevertheless, we think that is necessary to perform more detailed measures, mainly, in the near wake region in order to be able to follow the

spatial evolution of the generated vortex structures by the miniflap and their combination with the upcoming flow from the upper surface of the airfoil.

## 5. References

- Bacchi, F., Marañón Di Leo, J., Delnero, J. S., Colman, J., Martinez, M., Camocardi, M. & Boldes, U. 2006. Determinación experimental del efecto de mini flaps Gurney sobre un perfil HQ-17. *Fluidos-2006 IX Reunión Sobre Recientes Avances En Física de Fluidos y sus Aplicaciones*, Mendoza, Argentina.
- Bloy, A.W. & Durrant, M.T. 1995. Aerodynamic Characteristics of an aerofoil with Small Trailing Edge Flaps. *Wind Engineering*, Vol. 19, No.3, pp 167-172.
- Boldes, U.; Delnero, J.; Marañón Di Leo, J.; Colman, J.; Camocardi, M. & François, D. 2008. Influencia en la sustentación, de los vórtices de la estela de un perfil con miniflap tipo Gurney. Actas 1er Congreso Nacional de Ingeniería Aeronáutica. La Plata, Argentina.
- Gai, S. L. & Palfrey, R. 2003 Influence of Trailing-Edge Flow Control on Airfoil Performance. *Journal of Aircraft*, Vol. 40, No. 2, pp. 332-337.
- Giguère, P., Lemay, J. & Dumas, G. 1995 Gurney Flap Effects and Scaling for Low-Speed Airfoils. AIAA Paper 95-1881, 13th AIAA Applied Aerodynamics Conference San Diego.
- Hah, C. & Lakshminarayana, B. 1982 Measurement and prediction of mean velocity and turbulence structure in the Near wake of an airfoil. *Journal of Fluid Mechanics*. Vol.115, pp. 251-282.
- Hinze, J.O. 1975 *Turbulence*. McGraw-Hill Mechanical Engineering.
- Li, Y., Wang, J. & Zhang, P. 2002 Effects of Gurney Flaps on a NACA 0012 Airfoil. *Flow, Turbulence and Combustion*, Vol. 68, No. 1, pp. 27-39.
- Liebeck, R.H. 1978 Design of subsonic airfoils for high lift. *Journal of Aircraft* Vol. 15, No. 9, pp 547-561.
- Matalanis, C.G. & Eaton, J.K. 2007 . Wake vortex alleviation using rapidly actuated Segmented Gurney flaps. Report 102. Flow Physics and Computation Division, Department of Mechanical Engineering, University of Stanford.
- Myose, R., Papadakis, M., & Heron, I. 1998. Gurney Flap Experiments on Airfoils, Wings, and Reflection Plane Model. *Journal of Aircraft*, Vol. 35, No. 2, pp. 206-211.
- Neuhart, D.H. & Pendergraft, O.C. 1988. A water tunnel study of Gurney flaps. NASA TM-4071.
- Storms, B.L. & Jang, C.S. 1994. Lift Enhancement of an Airfoil Using a Gurney Flap and Vortex Generators. *Journal of Aircraft* Vol. 31, No. 3, pp 542-547.
- Tang, D. & Dowel, E.H. 2007. Aerodynamic loading for an airfoil with an oscillating Gurney flap. *Journal of Aircraft*, Vol. 44, Nr. 4, pp. 1245-57.
- Van Dam, C. P., Yen, D. T. & Vijgen, P. M. H. W. 1999. Gurney Flap Experiments on Airfoil and Wings. *Journal of Aircraft*, Vol. 36, No. 2, pp. 484-486.
- Zhan, J. X. & Wang, J. J. 2004. Experimental Study of Gurney Flap and Apex Flap on a Delta Wing. *Journal of Aircraft*, Vol. 41, No. 6, pp. 1379-1383.